Poisson Noise Removal From Images Using the Fast Discrete Curvelet Transform

Sandeep Palakkal* and K.M.M. Prabhu†
Department of Electrical Engineering
Indian Institute of Technology Madras
Chennai – 600 036, India
Email: *sandeep.dion@gmail.com, †prabhu@ee.iitm.ac.in

***Abstract*—We propose a strategy to combine the variance stabilizing transform (VST), used for Poisson image denoising, with the fast discrete Curvelet transform (FDCT). The VST transforms the Poisson image to approximately Gaussian distributed, and the subsequent denoising can be performed in the Gaussian domain. However, the performance of the VST degrades when the original image intensity is very low. On the other hand, the FDCT can sparsely represent the intrinsic features of images having discontinuities along smooth curves. Therefore, it is suitable for denoising applications. Combining the VST with the FDCT leads to good Poisson image denoising algorithms, even for low intensity images. We present a simple approach to achieve this and demonstrate some simulation results. The results show that the VST combined with the FDCT is a promising candidate for Poisson denoising.**

***Index Terms*—variance stabilizing transform, fast discrete curvelet transform, nonsubsampled contourlet transform, Poisson denoising.**

I. Introduction

Poisson images occur in many situations where image acquisition is performed using the detection of particles, e.g., photons [1]. The signal-to-noise ratio (SNR) of such images is signal dependent and varies across the image plane. Variance stabilizing transforms (VST) such as the Anscombe VST [2] offer a pragmatic solution for Poisson noise removal. The VST stabilizes the variance of the Poisson image to a constant, and the resulting image tends to homoskedastic Gaussian as the intensity of the original image tends to infinity. This makes it possible to employ Gaussian-based denoising methods, which are, unlike Poisson denoising methods, well developed and widely employed. After denoising, the estimated image can be obtained by inverting the VST. A drawback of the VST is that when the intensity level of the input image is very low (i.e., at low SNRs), its performance deteriorates [3]. Multiscale VSTs (MS-VST), proposed in [3], combine the VST with the lowpass filters involved in various multiscale multidirection (MS-MD) transforms such as wavelets. The lowpass filters average out the noise to an extent thereby improving the SNR. Moreover, the MS-MD transforms sparsely capture the intrinsic geometry of an image. Due to these facts, MS-VST-based Poisson denoising methods yield good performance. In [3], MS-VSTs were developed for the wavelet, ridgelet and first generation curvelet transforms [4], and the curvelet was shown to yield the best performance. Recently, we have proposed [5] an MS-VST Poisson image denoising algorithm, based on the nonsubsampled contourlet transform (NSCT) [6]. We have shown that the NSCT, when combined with the VST, yields excellent Poisson denoising performance for low intensity images. Its performance is quite comparable to that of the curvelet, and it outperforms the wavelet by a large margin. The NSCT has less redundancy and computational complexity than the curvelet.

In this paper, we propose a strategy to combine the MS-VST with the second generation curvelet transform, specifically the fast discrete curvelet transform (FDCT) [7]. The FDCT is far less redundant than the NSCT. We apply our proposed FDCT-based MS-VST to denoise Poisson images and demonstrate a few preliminary results. We note that more experiments are to be conducted to arrive at a complete conclusion on the performance of the proposed method. However, the preliminary results show that the FDCT-based MS-VST is indeed a promising candidate for Poisson noise removal.

This paper is organized as follows. Section II briefly discusses the MS-VST. In Section III, we provide a brief overview of the implementation of FDCT. The proposed FDCT-based MS-VST is developed in Section IV. The steps involved in Poisson noise removal by using the MS-VSTs is outlined in Section V. Some simulation results are presented in Section VI, and Section VII concludes the paper.

II. Multiscale Variance Stabilizing Transform

Let $X = (X_i)_{i\in\mathbb{Z}^2}$, be an observed $N \times N$ Poisson noisy image. Each pixel value X_i is an independent Poisson random variable, i.e., $X_i \sim \mathcal{P}(\lambda_i)$. The mean λ_i of the Poisson variable X_i represents the true intensity of the i-th pixel, and the variance $\sigma_i^2 = \lambda_i$ of X_i can be considered as noise [1]. The SNR at i-th pixel is λ_i, and therefore, it is intensity dependent. The denoising problem aims to estimate the underlying true intensity profile $(\lambda_i)_{i\in\mathbb{Z}^2}$ of the image.

The performance of the VST is improved for low intensity images by preprocessing the input image using a lowpass filter. Let Y be the filtered Poisson image and h be the impulse response of the filter, which is assumed to be of finite length (FIR). Define $\tau_k = \sum_i (h[i])^k$, for $k = 1, 2, \ldots$, and assume that the image is locally homogeneous, i.e., $\lambda_{j-i} = \lambda$, for all i within the support of h. The VST for a filtered image is

defined [3] as

$$T(Y) \triangleq b \cdot \operatorname{sign}(Y + c)\sqrt{|Y + c|}\,, \tag{1}$$

where sign is the signum function. With the constants b and c defined as

$$b \triangleq 2\sqrt{|\tau_1|/\tau_2} \quad \text{and} \quad c \triangleq \frac{7\tau_2}{8\tau_1} - \frac{\tau_3}{2\tau_2}\,, \tag{2}$$

it was shown in [3] that

$$T(Y) - b \cdot \operatorname{sign}(\tau_1)\sqrt{|\tau_1|\lambda} \xrightarrow[\lambda \to +\infty]{\mathcal{D}} \mathcal{N}(0, 1) \tag{3}$$

and the rate of convergence of the variance of $T(Y)$ is $\mathcal{O}(\lambda^{-2})$. Using this concept, the VST defined in (1) was combined with the lowpass filters of various MS-MD transforms so that the transform coefficients asymptotically approach a Gaussian distribution [3]. A Poisson denoising algorithm using the MS-VST typically consists of the following three processing stages [3]:

1) **Transformation:** MS-VST is applied to the Poisson image. The resulting coefficients are approximately Gaussian distributed with constant variance. The variance depends solely on the MS-MD transform used.
2) **Detection:** A statistical hypothesis test is used to detect the significant coefficients in the subbands.
3) **Estimation:** Since the MS-VST is nonlinear, a direct inversion is not possible. Therefore, the denoised image is recovered using ℓ_1 optimization techniques.

III. Fast Discrete Curvelet Transform

The curvelet transforms, first generation [4] as well as second generation [8], provide a near-optimal sparse representation for images having discontinuities along C^2 (twice differentiable) curves. Two separate digital implementation of the second generation curvelets were proposed in [7]. They are (i) using the unequispaced fast Fourier transform (USFFT) and (ii) using frequency domain wrapping. Both implementations are conceptually the same. The common steps involved in both the implementations are outlined in Fig. 1. After computing the two-dimensional (2-D) discrete Fourier transform (DFT) of the image using the fast Fourier transform (FFT), curvelet frequency windows at different scales and angles are applied. By computing the 2-D inverse DFT (IDFT) of each windowed output, we obtain the curvelet coefficients. The image can be recovered without error from the curvelet coefficients by inverting each step involved.

Compared to the first generation curvelets, the FDCT is conceptually simpler, faster, and less redundant. The computational complexity of the FDCT is only $\mathcal{O}(N^2 \log N)$ for an $N \times N$ image. Its redundancy is about 7.2, whereas the first

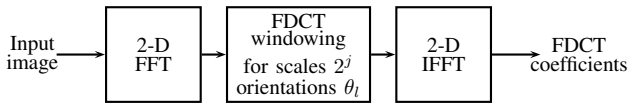

Fig. 1: The data flow in the forward FDCT

generation curvelet can be as highly redundant as $16J + 1$, where J is the number of curvelet scales. Similarly, when compared to the NSCT, the FDCT is less redundant and has more frequency resolution and better directionality properties [7].

The FDCT suffers from some drawbacks when used in denoising applications. Since the FDCT is compact in the frequency domain, it is more spread in the spatial domain. In our denoising experiments we have observed that the non-compactness of the curvelet functions introduces annoying oscillations in the reconstructed images, when nonlinear denoising techniques such as thresholding are employed; this is especially true when the SNR is very low. This phenomenon has been reported by other researchers as well, and a number of solutions — e.g., combine curvelet with other techniques — have been proposed in the literature. More discussion on this can be found in [9] and the references therein.

IV. MS-VST using the FDCT

The proposed scheme of combining the MS-VST with the FDCT is depicted in Fig. 2. In this scheme, prior to applying the 2-D DFT and FDCT windows, we decompose the image into a set of lowpass components using a 2-D filter bank having J channels. The first $(J-1)$ channels of the filter bank consists of 2-D lowpass filters. The passband of the filter in the $(J-j)$-th channel is $[-\pi/2^j, \pi/2^j]^2$. The J-th channel contains no lowpass filter. This arrangement decomposes the input image into an oversampled dyadic lowpass pyramid. Each lowpass output is stabilized to Gaussian by applying the MS-VST as defined in (1)–(2). Subsequently, 2-D DFT is applied to each lowpass band, and the FDCT windows of different orientations corresponding to the $2^{(J-j)}$-th scale is applied on the j-th lowpass component, for $j = 1, 2, \ldots J$. Taking the IDFT results in the detail coefficients of the FDCT. The lowpass FDCT window is applied to the J-th channel, in which there is no lowpass filter. This is done so that no error is introduced in the approximation coefficients. Moreover, we have chosen the proposed lowpass filter bank over the usual iterative Laplacian pyramid in order to avoid the cumulative errors in the passband due to iterative filtering. We note that the lowpass filters on the front end are superfluous as far as the FDCT is concerned, and they only facilitate the augmentation of MS-VST to the FDCT. Each lowpass component is multiplied with only those FDCT windows, which correspond to the associated scale. Therefore, the number of computations of the FDCT remains the same as that of the original version. But the overall number of computations increases because the 2-D DFT is computed in each channel of the filter bank. This is J times more when compared to the original FDCT algorithm. However, the overall computational complexity remains the same as $\mathcal{O}(N^2 \log N)$ for an $N \times N$ image.

From the discussion in Section II, it follows that the output of each MS-VST block in Fig. 2 is approximately Gaussian when the input is a Poisson image. Since the subsequent FDCT structure consists only of linear highpass filters, it follows that the FDCT coefficients are also approximately homoskedastic

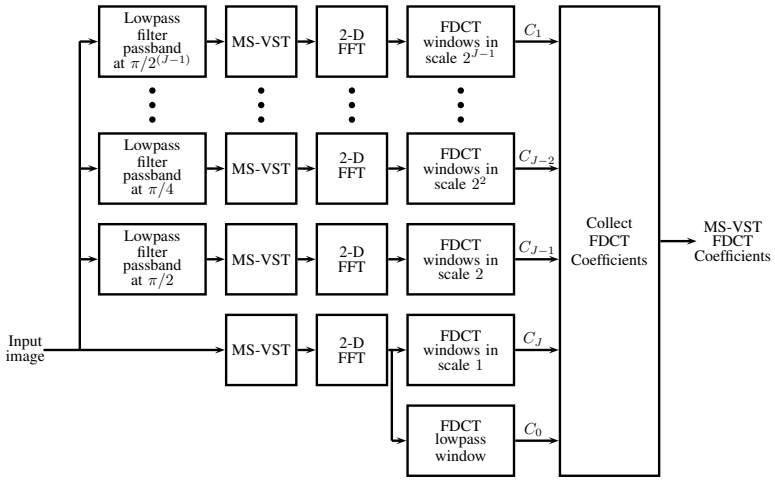

Fig. 2: Proposed FDCT-based MS-VST scheme

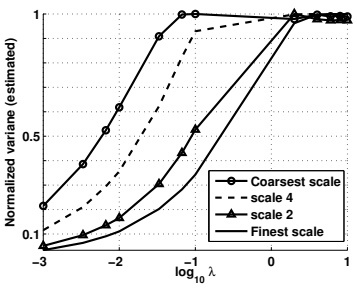

Fig. 3: Variance of MS-VST FDCT coefficients

Gaussian with zero mean. We have computed the variance of the FDCT coefficients obtained by the proposed scheme. We have used Monte Carlo simulations by giving the Poisson noise as inputs to the filter bank shown in Fig. 2. We have repeated this analysis for a range of low intensity images. The results for different curvelet scales are plotted in Fig. 3, in which the values of the variances are normalized to unity. It shows that the variance of the MS-VST+FDCT coefficients converge to a constant at low intensities. Also, because the coefficients in the coarser scales are obtained from lowpass filters with narrower passband, the SNR is improved more, and hence they converge faster.

Lowpass filter design: The additional filters used will cause errors in the FDCT coefficients and perhaps destroy its perfect reconstruction property. This does not cause a serious problem in the denoising applications because, as we explain in Section V, the FDCT coefficients obtained from the proposed structure are only used to obtain a multiresolution support $\mathcal{M}$ consisting of the locations of the significant FDCT coefficients. The reconstruction is performed by ℓ_1 optimization from the noisy image directly, but by making use of $\mathcal{M}$. Therefore, we only try to minimize the errors in the FDCT coefficients. To this end, we design linear-phase FIR filters by minimizing the maximum error in the passband. Our approach can be further justified as follows. Assume that we remove the MS-VST block in our filter bank structure given in Fig. 2. The resulting FDCT coefficients for an image X are given by

$$\overline{c}(j,l,k) = c(j,l,k) + c_\Delta(j,l,k)\,, \tag{4}$$

where $c(j,l,k)$ is the original FDCT coefficients of X, $c_\Delta(j,l,k)$ is the error introduced by the proposed structure, and j,l and k represent the FDCT scale, orientation and location, respectively. From [7], it follows that

$$c_\Delta(j,l,k) = \int \Delta_j(\omega)\widehat{X}(\omega)U_j(S_{\theta_l}^{-1}\omega)e^{i\langle S_{\theta_l}^{-T},\omega\rangle}d\omega\,. \tag{5}$$

where $\widehat{X}$ is the 2-D discrete-time Fourier transform of X, $\omega = (\omega_1,\omega_2)$ is the 2-D digital frequency, U_j is the curvelet window corresponding to the scale 2^j, and S is the shear matrix which determines the orientation of U in the frequency domain. In (5), $\Delta_j(\omega)$ is the error between the passband response of the j-th lowpass filter and its ideal value (i.e., unity). If $|\Delta(\omega)| \le \epsilon$, where $\epsilon > 0$, then

$$|c_\Delta(j,l,k)| = \epsilon \int |\widehat{X}(\omega)|U_j(S_{\theta_l}^{-1}\omega)d\omega \le \epsilon M\phi_j[0]\,, \tag{6}$$

where ϕ_j is the curvelet function in the space domain corresponding to U_j and M is the maximum value of $|\widehat{X}(\omega)|$. From (6), we note that by making ϵ arbitrarily small, we can minimize the error in the FDCT coefficients obtained by using the proposed structure for absolutely summable (i.e., bounded in the frequency domain) images. Since we need a passband which is supported inside a simple square in the 2-D frequency plane, we first design a one-dimensional linear-phase FIR filter and obtain the 2-D filter by simply taking its tensor product. During the implementation, we make the filter zero-phase by performing noncausal convolution. The one-dimensional filters can be designed by using methods such as Chebyshev equiripple approximation or maximally flat filter design.

V. MS-VST Denoising Algorithm

For Poisson image denoising using the MS-VST, we follow the same steps as described in [3]. We first apply the FDCT-based MS-VST for converting the Poisson image to approximately Gaussian. Then we perform hard thresholding to detect the significant FDCT coefficients for a prespecified false detection rate (FDR) [10]. The locations of the detected coefficients define an FDCT multiresolution support $\mathcal{M}$ [3] for the image. The true intensity image is estimated by minimizing the ℓ_1 norm of the FDCT coefficients, reindexed as a column vector, with the constraint that the resulting

Fig. 4: MS-VST Denoising of Poisson image Barbara, size 256x256; (a) True image, intensity $[0.9, 20]$; (b) Poisson noisy image; (c) MS-VST+Curvelet-I; (d) MS-VST+NSCT; (e) MS-VST+SNSCT; (e) MS-VST+FDCT.

image has nonnegative pixel values and the FDCT coefficients belonging to $\mathcal{M}$ are preserved. We solve this problem by using the hybrid steepest descent (HSD) algorithm [11], as adapted in [3].

To measure the performance of the MS-VST algorithms we use the normalised mean integrated squared error (NMISE), defined in [3]. For an $N \times N$ image, we compute the NMISE over thirty noisy realizations as

$$\text{NMISE} = \frac{1}{30} \sum_{n=1}^{30} \sum_{i=1}^{N^2} (\widehat{\lambda}_{in} - \lambda_i)^2 / \lambda_i \,, \tag{7}$$

where $\widehat{\lambda}_{in}$ is the estimate of λ_i from the n-th realization.

VI. Results and Discussion

We demonstrate a few denoising results obtained by the proposed MS-VST+FDCT for Poisson noisy images. We compare our method with other state-of-the-art MS-VST methods. The NMISE values for each method is tabulated in Table I; the redundancy factor of the methods for the number of scales and directions used are given inside the brackets. A few important specifications of our experiments are: five scales and $\{8, 16, 16, 32, 32\}$ directions (from coarse to fine) for the MS-MD transforms except the first generation curvelet, for which four scales are used; the FDCT implementation based on frequency wrapping; images of size 256×256 and intensity in the range $[0.9, 20]$; and FDR = 10^{-3} and number of iterations in HSD = 5 [3].

Figure 4 shows the results corresponding to the image *Barbara*. The MS-VST+NSCT (Fig. 4d) yields better visual performance by bringing out the high frequency details in the image with very less artifacts. In addition, it has the least NMISE value, as shown in Table I. Like the MS-VST+NSCT, the proposed method (Fig. 4f) is also successful to bring out the high frequency details, but its result contains a few ringing artifacts. This is partly due to the lesser redundancy and the inherent limitation of the FDCT to perform well in the denoising applications, as discussed in Section III. In terms of redundancy, FDCT is comparable with the semi-NSCT (SNSCT) (Fig. 4d), which is a semi nonsubsampled version of the NSCT [5], [6]. The NMISE obtained for our method is better than that for the SNSCT. Similarly, Fig. 5 shows the results obtained for the satellite image of the saturn rings[1]. For this image, the performance of our method comes close to the other methods. In fact, the NMISE is very close to that of the NSCT and better than that of the SNSCT. For both the images, Barbara and saturn rings, the proposed FDCT method yields performance comparable with the first generation curvelets.

While redundancy is favourable for denoising applications, the fact that our method performs as closely as the other state-of-the-art methods but with lower redundancy proves that it is a potential candidate for Poisson denoising. We believe that using a hybrid approach of combining the FDCT with other methods [9] will expand its potential use greatly.

[1]Courtesy NASA/JPL-Caltech. File name: PIA01531.

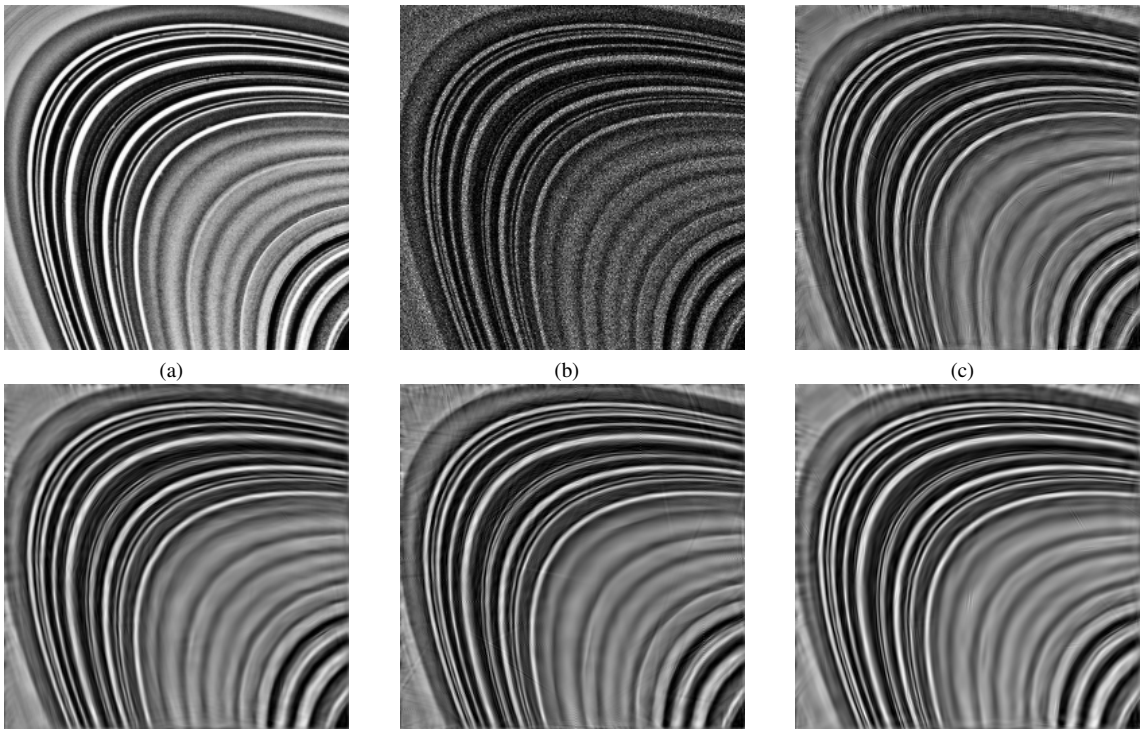

Fig. 5: MS-VST Denoising of Poisson image Saturn, size 256x256; (a) True image, intensity $[0.9, 20]$ (Courtesy NASA/JPL-Caltech); (b) Poisson noisy image; (c) MS-VST+Curvelet-I; (d) MS-VST+NSCT; (e) MS-VST+SNSCT; (f) MS-VST+FDCT

TABLE I: NMISE for different MS-VST methods

Method (redundancy)	**Barbara**	**Saturn**
MS-VST+Curvelet-I (65)	0.2035	**0.2413**
MS-VST+NSCT (105)	**0.1919**	0.2671
MS-VST+SNSCT (6)	0.2424	0.2713
MS-VST+FDCT (7.2)	0.2274	0.2667
MS-VST+Wavelet (16) *(results not shown)*	0.3057	0.3327

VII. Conclusion

We have presented an approach to combine the variance stabilizing transform (VST) with the fast discrete curvelet transform (FDCT), which can be used for Poisson image denoising. This method transforms the denoising problem from Poisson to Gaussian domain. Our approach to combine the VST with the FDCT is simple and straight forward, and slightly increases the number of computations in the FDCT. However, the overall computational complexity remains the same as that of the FDCT. Results of our Poisson denoising experiments promise that the combination of VST with FDCT is a potential candidate for future explorations.

Acknowledgement

S. P. wishes to thank his fellow researchers Sanjay K. Sindhi and Bharath H. N., IIT Madras, for their help and support during the preparation of this paper. The authors also would like to acknowledge the use of the Curvelab Toolbox prepared by D. L Donoho, and the NSCT Toolbox prepared by A. L. Cunha, for conducting the simulations given in this paper. In addition, the authors wishes to thank the anonymous reviewers for their valuable comments and suggestions.

References

[1] R. M. Willet, "Multiscale analysis of photon-limited astronomical images," in *Statistical Challenges in Modern Astronomy IV ASP Conf. Ser.*, vol. 371, Pennsylvania, USA, June 2006, p. 247.

[2] F. J. Anscombe, "The transformation of Poisson, binomial and negative-binomial data," *Biometrika*, vol. 35, pp. 246–254, 1948.

[3] B. Zhang, J. M. Fadili, and J.-L. Starck, "Wavelets, ridgelets, and curvelets for Poisson noise removal," *IEEE Trans. Image Process.*, vol. 17, pp. 1093–1108, July 2008.

[4] E. J. Candés and D. L. Donoho, "Curvelets – A surprisingly effective nonadaptive representation for objects with edges," in *Curve and Surface fitting*. Nashville, TN: Vanderbilt Univ. Press, 2000, pp. 105–120.

[5] S. Palakkal and K. M. M. Prabhu, "Contourlet-based variance stabilising transform for Poisson denoising," *IET Image Process.*, submitted for publication.

[6] A. L. da Cunha, J. Zhou, and M. N. Do, "The nonsubsampled contourlet transform: Theory, design, and applications," *IEEE Trans. on Image Process.*, vol. 15, pp. 3089–3101, Oct. 2006.

[7] E. Candes, L. Demanet, D. Donoho, and L. Ying, "Fast discrete curvelet transforms," *SIAM Multiscale Modeling and Simulation*, vol. 5, no. 3, pp. 861–899, 2006.

[8] E. J. Candés and D. L. Donoho, "New tight frames of curvelets and optimal representations of objects with piecewise C^2 singularities," *Commun. on Pure and Appl. Math.*, vol. LVII, pp. 0219–0266, 2004.

[9] J. Ma and G. Plonka, "The curvelet transform," *IEEE Signal Process. Mag.*, vol. 27, pp. 118 –133, Mar. 2010.

[10] Y. Benjamini and Y. Hochberg, "Controlling the false discovery rate: A practical and powerful approach to multiple testing," *J. Roy. Stat. Soc. B*, vol. 57, no. 1, pp. 289–300, 1995.

[11] I. Yamada, "The hybrid steepest descent method for the variational inequality problem over the intersection of fixed point sets of nonexpansive mappings," in *Inherently parallel algorithm in feasibility and optimization and their applications*. New York: Elsevier, 2001.